Development 123, 81-93 (1995)
Printed in Great Britain © The Company of Biologists Limited 1996
DEV3378

Genes establishing dorsoventral pattern formation in the zebrafish embryo: the ventral specifying genes

Mary C. Mullins*, Matthias Hammerschmidt†, Donald A. Kane‡, Jörg Odenthal, Michael Brand§, Fredericus J. M. van Eeden, Makoto Furutani-Seiki, Michael Granato, Pascal Haffter, Carl-Philipp Heisenberg, Yun-Jin Jiang, Robert N. Kelsh‡ and Christiane Nüsslein-Volhard

Max-Planck-Institut für Entwicklungsbiologie, Spemannstrasse 35/III, 72076 Tübingen, Germany

*Author for correspondence at present address: University of Pennsylvania, Department of Cell and Developmental Biology, 605 Stellar-Chance, Philadelphia, PA 19104-6058, USA (e-mail: mullins@mail.med.upenn.edu)
†Present address: Harvard University, 16 Divinity Avenue, Cambridge, Massachusetts 02138, USA
‡Present address: University of Oregon, Insitute of Neuroscience, Eugene, Oregon 97403, USA
§Present address: Institut für Neurobiologie, Universität Heidelberg, Im Neuenheimer Feld 364, 69120 Heidelberg, Germany

SUMMARY

We identified 6 genes that are essential for specifying ventral regions of the early zebrafish embryo. Mutations in these genes cause an expansion of structures normally derived from dorsal-lateral regions of the blastula at the expense of ventrally derived structures. A series of phenotypes of varied strengths is observed with different alleles of these mutants. The weakest phenotype is a reduction in the ventral tail fin, observed as a dominant phenotype of *swirl*, *piggytail*, and *somitabun* and a recessive phenotype of *mini fin*, *lost-a-fin* and some *piggytail* alleles. With increasing phenotypic strength, the blood and pronephric anlagen are also reduced or absent, while the paraxial mesoderm and anterior neuroectoderm is progressively expanded. In the strong phenotypes, displayed by homozygous embryos of *snailhouse*, *swirl* and *somitabun*, the somites circle around the embryo and the midbrain region is expanded laterally.

Several mutations in this group of genes are semidominant as well as recessive indicating a strong dosage sensitivity of the processes involved. Mutations in the *piggytail* gene display an unusual dominance that depends on both a maternal and zygotic heterozygous genotype, while *somitabun* is a fully penetrant dominant maternal-effect mutation. The similar and overlapping phenotypes of mutants of the 6 genes identified suggest that they function in a common pathway, which begins in oogenesis, but also depends on factors provided after the onset of zygotic transcription, presumably during blastula stages. This pathway provides ventral positional information, counteracting the dorsalizing instructions of the organizer, which is localized in the dorsal shield.

Key words: dorsalized mutant, dorsoventral axis, ventral determination, pattern formation, maternal effect, gastrulation, tailbud, zebrafish

INTRODUCTION

The pattern formation mechanisms establishing the body plan of vertebrates is best understood in *Xenopus laevis*. The dorsoventral axis of the frog is visible shortly after fertilization by rotation of the surface cortex and formation of the grey crescent (reviewed by Sive, 1993). By an unknown mechanism, this cortical rotation results in the local activation (or repression) of a maternal factor on the future dorsal side. This dorsally localized activity, the Nieuwkoop center, resides in the vegetal blastomeres and during the blastula stage induces overlying marginal blastomeres to form dorsal mesoderm, the future Spemann organizer. Similarly, ventral and lateral vegetal cells induce overlying marginal blastomeres to form ventral mesoderm. A further refinement of dorsoventral patterning occurs following the midblastula transition. The Spemann organizer (the induced dorsal mesoderm) produces a signal, which patterns adjacent mesoderm to form muscle and induces the neuroectoderm to form at anterior-dorsal positions (for reviews see Kessler and Melton, 1994; Sive, 1993; Kimelman et al., 1992). An additional ventral signal is implicated in inhibiting this dorsal signal and specifying ventral cell fates (reviewed in Harland, 1994).

Numerous molecules have been proposed to play roles in these signalling events. Members of the TGFβ and the FGF families are candidates for the signals derived from the vegetal pole (for review see Slack, 1994), while the products of genes such as *noggin* (Lamb et al., 1993; Smith et al., 1993), *chordin* (Hemmati-Brivanlou et al., 1994; Sasai et al., 1994, 1995), and *follistatin* (Kessler and Melton, 1995; Sasai et al., 1995), and those of the *wnt* gene family members (Cui et al., 1995; Ku and Melton, 1993; Smith and Harland, 1991) have been implicated in the dorsalization signalling and neural induction processes.

Another signalling molecule, bone morphogenetic protein-4 (BMP-4) of the TGFβ family, has been shown to be particu-

larly important with respect to dorsoventral patterning of the mesoderm. Ectopic expression of BMP-4 in dorsal blastomeres results in a ventralization of the embryo: a reduction of dorsal tissues accompanied by an expansion of ventral cell types (Dale et al., 1992; Jones et al., 1992). Consistent with this finding, expression of a dominant negative form of a BMP receptor (Suzuki et al., 1994; Maeno et al., 1994; Graff et al., 1994; Schmidt et al., 1995a) or BMP-4 (Hawley et al., 1995), or injection of antisense *BMP-4* RNA (Steinbeisser et al., 1995) into *Xenopus* embryos results in a dorsalization of ventral mesoderm. Additionally, BMP-4 has the ability to induce ventral mesoderm in animal cap assays (Köster et al., 1991; Dale et al., 1992; Jones et al., 1992; Hemmati-Brivanlou and Thomsen, 1995; Schmidt et al., 1995a). Mouse embryos mutant for the BMP receptor do not form any mesoderm (Mishina et al., 1995). Similarly, most *BMP-4* mutant mice do not form mesoderm and arrest at the egg cylinder stage; however, some mutant embryos develop beyond this stage and exhibit a disorganization or truncation of posterior structures and a reduction in ventral-lateral mesoderm (Winnier et al., 1995). These results implicate *BMP-4* and the BMP receptor in mesoderm formation and ventral and posterior cell fate determination. As *BMP-4* and the BMP receptor mRNAs are expressed both maternally and zygotically in *Xenopus* (Köster et al., 1991; Dale et al., 1992; Graff et al., 1994) their ventralizing action could be a part of the ventrovegetal center and/or a postblastula stage ventral activity that inhibits the dorsalizing signal of Spemann's organizer (see Harland, 1994 for a review). While the maternal transcripts of both genes are not localized in the embryo, *BMP-4* mRNA becomes restricted to ventral and lateral regions during gastrulation (Fainsod et al., 1994; Schmidt et al. 1995a; Hemmati-Brivanlou and Thomsen, 1995).

Considerably less is known about mesoderm induction and dorsoventral pattern formation in the zebrafish. An equivalent of the cortical rotation is not apparent in the fish zygote and the orientation of the dorsoventral axis does not become evident until shortly before gastrulation (Schmitz and Campos-Ortega, 1994). During gastrulation, involution and dorsal convergence lead to the formation of a bilayered embryo with a prominent thickening at its dorsal side, termed the embryonic shield (see Kimmel et al., 1995, for a staging series). It has been demonstrated that shield cells, when transplanted to an ectopic position, are able to induce a secondary axis (Ho, 1992). Thus, the shield appears to function as the Spemann organizer in the early zebrafish gastrula. The molecular events involved in establishing the shield are unclear, although a number of experiments suggest the yolk cell to be a source of inductive signals (Devillers, 1952; Kostomarova, 1969; Oppenheimer, 1936).

As in *Xenopus*, LiCl treatment of early cleavage stage zebrafish embryos causes a dorsalization of the embryo (Joly et al., 1993; Stachel et al., 1993), suggesting a common early pathway of dorsal induction in zebrafish and *Xenopus*. This notion is strengthened by the similarity of the fate maps of *Xenopus* (Dale and Slack, 1987) and zebrafish embryos (Kimmel et al., 1990): the notochord and head mesoderm, for example, map to the most dorsal marginal region of the blastoderm, somitic mesoderm encompasses a large portion of the lateral and ventral marginal zone, and pronephros and blood precursors are derived from ventrolateral and ventral positions, respectively. In both zebrafish and *Xenopus*, more posterior tissues are generally derived from more ventral regions in the blastoderm. For example, tail progenitor cells primarily arise from the ventral side of the blastoderm. Many vertebrate genes that are expressed at blastula or early gastrula stages have been cloned by homology in zebrafish and have similar expression patterns to their mouse or frog counterparts suggesting that determination processes are conserved between these vertebrates.

The functional assays used in amphibians have been extremely valuable for identifying genes with properties expected of mesoderm inducers or dorsalizing and ventralizing signals. However, they do not reveal whether the identified molecules function in this manner endogenously in the embryo. The most stringent test for a gene playing an essential role in a biological process is the analysis of mutants of this gene. This approach has been used successfully in mice to examine the function of a number of genes during early development, including *nodal* (Conlon et al., 1994), *HNF-3β* (Ang and Rossant, 1994; Weinstein et al., 1994), *FGFR* (Deng et al., 1994; Yamaguchi et al., 1994), *Brachyury* (Herrmann and Kispert, 1994; Beddington et al., 1992), *lim1* (Shawlot and Behringer, 1995) and *BMP-4* (Hogan et al., 1994; Winnier et al., 1995). Some of these genes are involved in formation of mesoderm and posterior pattern, but only *BMP-4* has been reported to be involved in dorsoventral patterning of the early gastrula (Winnier et al., 1995).

Here we describe the identification of 22 mutants that show reductions in ventrally derived structures and expansions in dorsal tissues in the zebrafish embryo. These mutants define 6 genes, 3 of which contain multiple alleles. *piggytail* (*pgy*), and possibly *somitabun* (*sbn*), function maternally and zygotically in the establishment of the dorsoventral axis, while *swirl* (*swr*), *snailhouse (snh)*, *lost-a-fin (laf)*, and *mini fin* (*mfn*) appear to function only zygotically. Embryos mutant in all 6 genes show abnormal gastrulation movements. The products of these genes are good candidates for molecules contributing to a ventralizing factor(s) that inhibits the dorsalization signal emanating from the organizer.

MATERIALS AND METHODS

Fish procedures and genetics

Breeding and maintenance of fish and identification and isolation of mutants was done as described by Mullins et al. (1994) and Haffter et al. (1996). The following mutants were used for photography of live animals and staining, except where otherwise noted: laf^{tm110b} and pgy^{dty40} as representative of *laf and pgy*, respectively, and swr^{ta72} of *swr*, except for the embryos in Figs 3F and 4K which were swr^{tc300}.

Antibody staining and whole mount in situ hybridization

In situ hybridization and antibody staining were done as described by Schulte-Merker et al. (1992). The RNA probes that were used were *myoD* (Weinberg et al., 1996), *gata1* (Detrich et al., 1995), *eve1* (Joly et al., 1993), *pax2* (Krauss et al., 1991b) and *fkd3* (J. O., unpublished results). Antibodies that were used were an anti-Ntl rabbit polyclonal antiserum (Schulte-Merker et al., 1992). Embryos were photographed using a Zeiss Axiophot microscope. Pictures were scanned into a Macintosh computer using a Nikon slidescanner and processed using Adobe photoshop software.

Blood staining

Histological staining for blood was done as described by Iuchi and Yamamoto (1993).

RESULTS

In our large-scale screen for visible embryonic mutants we identified a total of 22 mutants, which display progressive reductions in the ventral tail fin, length of the tail and amount of blood, associated with progressive expansions of somitic mesoderm. Complementation tests have placed 18 of the mutants into 5 complementation groups, *swirl* (*swr*), *snailhouse (snh), piggytail* (*pgy*), *lost-a-fin (laf),* and *mini fin* (*mfn*), while the analysis is not yet complete for 3 mutants and inconclusive for 1 mutant, which is tentatively called *somitabun* (*sbn*) (Table 1 and see below). A spectrum of phenotypes is observed among the mutants, with indistinguishable mutant phenotypes found for the alleles of more than one gene (Table 2). For the ease of describing the genes, we grouped the mutant phenotypes according to their strength into 5 classes, with 1 being the weakest and 5 the strongest. The strength of the phenotype is based on the degree to which the notochord, somites and tail are affected.

The series of phenotypes

The strongest class of defects, class 5, is displayed in homozygous *swr* and *sbn* embryos. At 70% epiboly a thinning of the wild-type gastrula occurs in ventral anterior regions as a result of epiboly and dorsal convergence (80% is shown in Fig. 1A, Warga and Kimmel, 1990). Class 5 mutant embryos are identifiable at this stage by a thickened ventral side (Fig. 1E), probably due to reduced dorsal convergence. At the bud stage, the embryo is ovoid rather than round and the notochord appears broadened (Fig. 1B,F). The phenotype becomes very striking at somite stages as the somites extend from the notochord around the circumference of the embryo fusing on the ventral side (Fig. 1C,G). The tailbud does not proceed around the yolk toward the ventral side, as in wild-type embryos, but instead extends off the yolk (Fig. 1C,G). This could reflect an attempt of the vegetal cells around the circumference of the embryo to extend around the yolk, which would normally be exhibited only by the dorsally lying cells

Table 1. Dorsalized mutants

Gene (no. of alleles)	Alleles	Recessive phenotype (Class)†	Genetic features
swirl (2)	*tc300*	C5	Recessive
	ta72	C5	Zygotic semidominant
somitabun (1)	*dtc24*	C5	Maternal dominant, zygotic semidominant
snailhouse (1)	*ty68a*	C4	Recessive
piggytail (6)	*dty40*	C3 and C4	Maternal/zygotic dominant
	dti216	C2 and C3	Maternal/zygotic semi-dominant
	tc227a	C1 and C2	Maternal/zygotic semi-dominant
	tm124a	C1	Recessive
	ta206	C1	Recessive
	tx223	C1	Recessive
lost-a-fin (1)	*tm110b*	C2	Recessive
mini fin (8)	*tv9b*	C1	Recessive
	tc263a	C1	Recessive
	tt203a	C1	Recessive
	ty130a	C1	Recessive
	tb241c	C1	Recessive
	tf211a	C1	Recessive
	tf215a	C1	Recessive
	tn217b	C1	Recessive
Unresolved* (3)	*dty236b*	variable‡	Semidominant
	dtm13c	(C2§)	Dominant
	tf18c	C1	Recessive

*Complementation testing is not complete for the unresolved mutants.

†Phenotypic strength is defined in the text using a series from class 1 (C1) to class 5 (C5) with class 5 being the strongest phenotype and class 1 the weakest. Representatives of each class are shown in Fig. 1 and 2.

‡*dty236b* mutant embryos vary in phenotype: C1, C3 and C5 phenotypes, in addition to various other phenotypes have been observed.

§*dtm13c* was recently identified in the background of another mutant. Only carrier females have been identified, which produce in 25-50% of their progeny a dominant C2 phenotype.

Table 2. Percentage phenotypic classes produced by mutant crosses

Cross female × male	Total*	*n*	%Normal	%C1	%C2	%C3	%C4	%C5
swirl								
tc300a/+ × *tc300a*/+	3	230	76	0	0	0	0	24
ta72/+ × +/+	2	240	54	30	16	0	0	0
	1	28	61	39	0	0	0	0
+/+ × *ta72*/+	1	44	57	23	20	0	0	0
	1	60	87	13	0	0	0	0
	1	50	98	2	0	0	0	0
ta72/+ × *ta72*/+	3	554	38	34	3	0	0	25
somitabun								
dtc24/+ × +/+	3	240	0	0	0	0	100	0
+/+ × *dtc24*/+	1	96	61	39	0	0	0	0
	1	80	56	34	10	0	0	0
	1	138	85	15	0	0	0	0
dtc24/+ × *dtc24*/+	3	271	0	0	0	0	68	32
tc300/+ × *dtc24*/+	1	61	54	25	3	18	0	0
	1	16	44	31	6	0	19	0
ta72/+ × *dtc24*/+	1	120	18	16	20	12	27	7
	1	118	47	27	1	25	0	0
	1	44	41	29.5		0	29.5	0
tc227a/+ × *dtc24*/+	1	165	50	0	15	35	0	0
	2	331	41	6	11	41	0	0
snailhouse								
ty68a/+ × *ty68a*/+	2	206	75	0	0	0	25	0
	1	80	72.5	0	0	27.5	0	0
piggytail								
dty40/+ × +/+	1	525	50	36	13	0	0	0
	1	118	34	25	41	0	0	0
	1	172	66	23	12	0	0	0
+/+ × *dty40*/+	3	160	100	0	0	0	0	0
dty40/+ × *dty40*/+	3	344	23	33	24	21	2	0
dti216/+ × +/+	1	92	86	14	0	0	0	0
+/+ × *dti216*/+	1	40	100	0	0	0	0	0
dti216/+ × *dti216*/+	2	90	52	29	11	8	0	0
tc227a/+ × +/+	1	80	98	2	0	0	0	0
	2	160	88	12	0	0	0	0
+/+ × *tc227a*/+	1	20	100	0	0	0	0	0
tc227a/+ × *tc227a*/+	3	205	65	10	25	0	0	0
tx223b/+ × *tx223b*/+	3	214	79	21	0	0	0	0
lost-a-fin								
tm110b/+ × *tm110b*/+	2	170	75	0	25	0	0	0
mini fin								
tc263/+ × *tc263*/+	3	256	76	24	0	0	0	0

*The total number of crosses scored. Counts from different crosses are shown to illustrate the observed variability. When the frequency of the phenotypic classes was similar between egg lays, then the numbers were pooled.

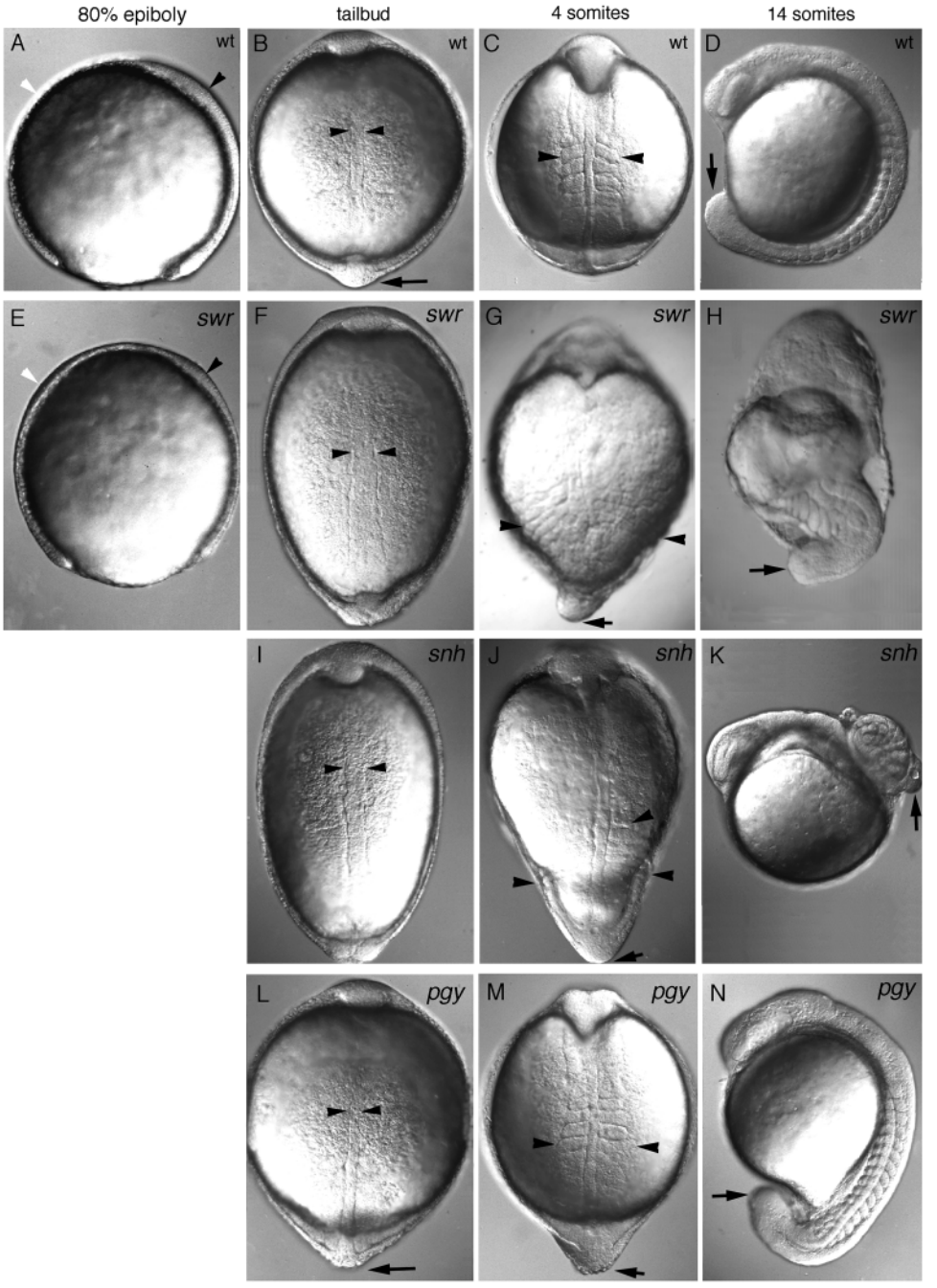

Fig. 1. Morphological defects visible in live mutant gastrulae of *swr*, *snh* and *pgy*. Dorsal is to the right in lateral views and animal pole is up in dorsal views. (A-D) Wild type, (E-H) *swr* (class 5 phenotype), (I-K) *snh* (class 4 phenotype), (L-N) *pgy* (class 3 phenotype). A lateral view of an 80% epiboly stage wild-type (A) and *swr* mutant (E) embryo showing the thickened ventral side (white arrowhead) and thinner dorsal axis (black arrowhead) in *swr*. A dorsal view at bud stage of wild-type (B), *swr* (F), *snh* (I), and *pgy* (L) embryos (the notochord is delineated by arrowheads). Dorsal views of 4-somite stage embryos: wild-type (C), *swr* (G), *snh* (J), and *pgy* (M). The most lateral extent of the somites is marked by arrowheads; an arrow indicates the position of the tailbud, which is not visible in the wild type (C) because it has extended around the yolk. (D,H,K,N) Lateral views of 14-somite stage embryos: wild-type (D), *swr* (H), *snh* (K), and *pgy* (N) (the tailbud is indicated with an arrow).

(Kimmel et al., 1995). A narrowing of the circumference of the embryo occurs in posterior regions, probably caused by the somites circling around the embryo. As a consequence, the yolk becomes extruded anteriorly. This posterior constriction of the embryo and anterior expulsion of the yolk becomes more severe as development proceeds. The increased amount of yolk now present in the anterior part of the embryo appears to cause too great a hydrostatic pressure, so that by the 13 somite stage the yolk spills out of the embryo and the embryo lyses (Fig. 1H).

The second strongest mutant phenotype, class 4, is found in homozygous *snh* and dominant *sbn* mutant embryos (Table 2). As with class 5 mutants, the shape of the embryo becomes ovoid just prior to the bud stage, the notochord is broader (Fig. 1I), and the tailbud extends off the yolk prematurely (Fig. 1J). The first 2 somites are expanded laterally, but do not extend to ventral positions (as with class 5 embryos), whereas the posterior somites do (Fig. 1J). The posterior constriction in class 4 mutants does not lead to a bursting of the embryo, probably because the anterior somites are not as strongly expanded as in class 5 mutants. In later segmentation stages, the trunk axis twists around itself, like a snail shell (compare Fig 1D,K). Two tissues of ventral origin in the blastoderm, the tail and blood are not apparent, (Fig. 2A,B), although small amounts of blood can be detected in some mutant embryos in a histological stain (data not shown). The anteriormost region

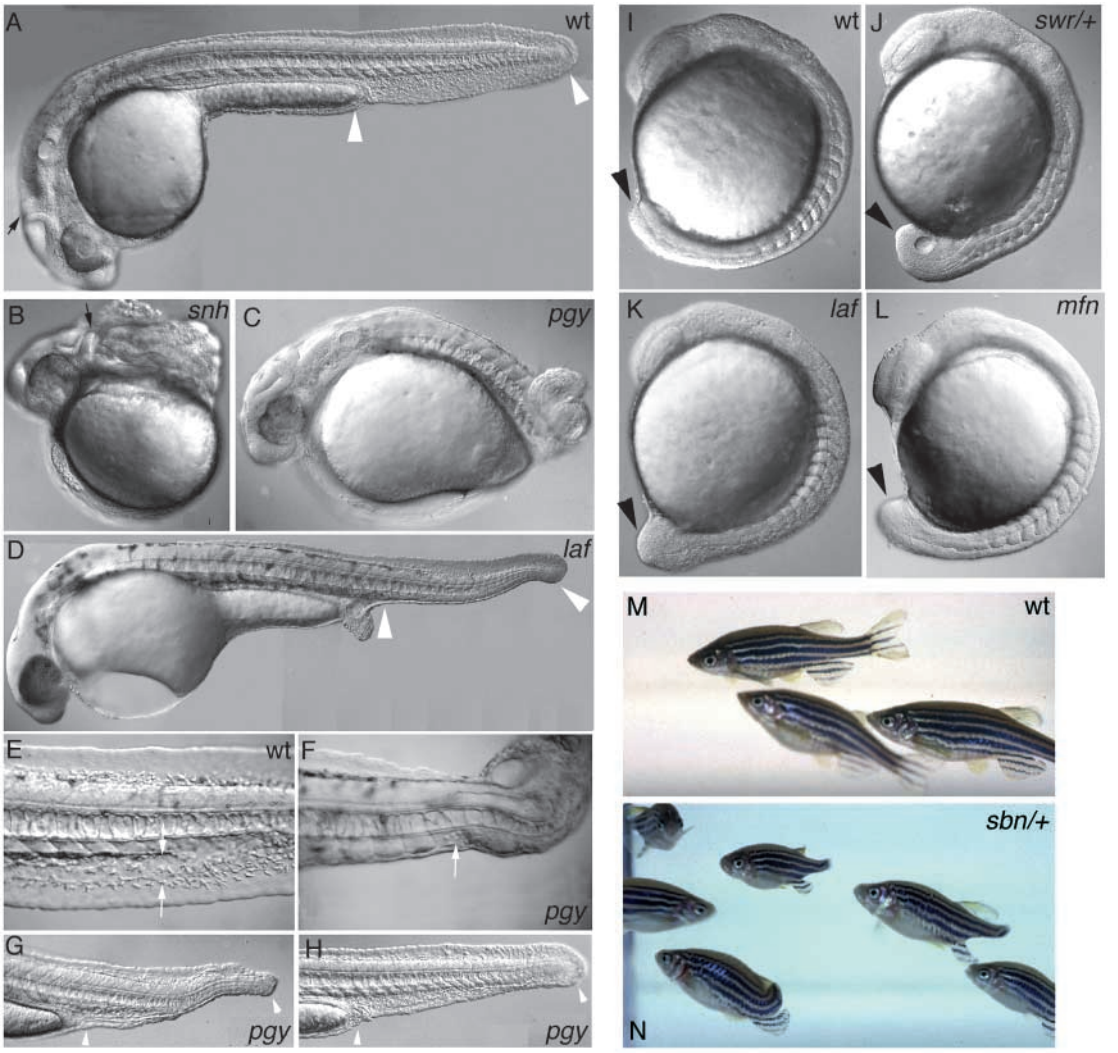

Fig. 2. Live wild-type and mutant embryos at the 10-somite stage, day 1, and as adults. Lateral view of 1-day old embryos: wild type (A), *snh* (class 4) (B), *pgy* (class 3) (C), and *laf* (class 2) (D). A black arrow marks the midbrain/hindbrain boundary in A and B, and white arrowheads indicate the position of the ventral tail fin in A,D,G,H. An enlargement of part of the tail in a wild-type and a *pgy* mutant embryo is shown in E,F. The white arrows in E mark the position of the ventral tail vein, which is absent in F. Due to the absence of circulation in *pgy* mutants, stagnant blood cells are visible (white arrow in F). Tail of a pgy^{dty40} heterozygote (G) and a homozygote with a weak *pgy* allele (H), which are representative of class 1 phenotypes. Lateral views of 10-somite stage embryos: wild type (I), *swr*/+ (class 2; J), *laf* (class 2; K), and *mfn* (class 1; L). The black arrowhead in I-L marks the tailbud. Wild-type adults (M) and class 1 mutants as adults (N). Note the absence of the tail fin, partial deletion of the anal fin, and short tail in some adults in N.

of the embryo is comparatively normal; the eyes are developed and the midbrain-hindbrain boundary of the brain is visible (Fig. 2B). However, other structures of the head are disorganized and the otic placodes are found fragmented at various positions on the yolk sac (data not shown). Additionally, the pectoral fin buds are improperly located on the yolk sac. The heart tubes are not joined at the midline and two beating heart chambers, often consisting of only a few beating cells, are seen in more lateral positions (data not shown). The embryos survive for 2 to 3 days and then necrose and die. A dorsalization of the embryo is strongly suggested by the phenotype of class 4 mutant embryos: a reduction in cell types of ventral origin in the blastoderm (blood and tail) and an expansion of dorsally derived tissues (anterior somites and notochord).

A phenotype of intermediate strength, class 3, is represented by homozygous mutant embryos of the strongest *pgy* allele, pgy^{dty40}. The mutant phenotype is visible at the bud stage as a slight protrusion of the tailbud (Fig. 1L). In early somite stages the phenotype is apparent as an enlarged tailbud that remains in a more vegetal position rather than extending around the yolk (Fig. 1M,N), similar to class 4 and 5 mutants. The anterior somites in class 3 mutant embryos are expanded laterally (Fig. 1M), but only beginning with somite 11 do the somites circle around the embryo (data not shown). In class 5 and 4 embryos this circling begins with the first and third somite, respectively. In contrast to class 4 mutants, the tail of class 3 mutants is present, but shortened and twisted (Fig. 2C) and the ventral tail vein and fin are missing (Fig. 2E,F). Blood is reduced in amount (data not shown). Blood circulation does not occur in 1-day old embryos as in wild type, probably due to the absence

of the ventral tail vein. Class 3 mutant embryos necrose and die by day 3. Although a less strong phenotype than class 4, the class 3 phenotype is also suggestive of a dorsalization of the embryo: a reduction in blood and tail length and an expansion of somitic mesoderm.

A weak phenotype, restricted to the tail region of the embryo, is displayed by embryos carrying the recessive alleles of *laf* and *mfn*, weak alleles of *pgy* and the dominant alleles of *pgy*, *swr*, and *sbn* (see Table 2). We distinguish two weak phenotypic classes. The class 2 phenotype is developed in mutants homozygous for *laf* and some *pgy* alleles (Table 1). The phenotype is visible by the 3 somite stage as a slight enlargement of the tailbud, which becomes more pronounced in later somite stages (Fig. 2I-K). As in class 3 mutants, the tailbud does not extend around the yolk as far as in the wild type, but lies in a more vegetal position and becomes enlarged (Fig. 2I,K). The tail is of about normal length, while the ventral tail vein and fin are missing (Fig. 2D). The embryos do not develop blood circulation, which likely results in failure of brain ventricle formation seen in many embryos (Fig. 2D). The mutant embryos necrose and die by day 3.

The class 1 phenotype is the weakest and is displayed in mutants homozygous for *mfn*, those with weak alleles of *pgy*, and dominant alleles of *pgy*, *swr*, and *sbn* (see Table 2). In these mutant embryos the ventral tail vein is present, while the ventral tail fin is entirely or partially absent (Fig. 2G,H). In other respects, the class 1 phenotype is very similar to that of class 2 embryos (Fig. 2L). Many of the embryos with weak phenotypes survive to adulthood and frequently have a short tail and no tail fin (Fig. 2M,N).

Expanded expression domains of mesodermal genes toward lateral and ventral regions

We investigated the phenotypes in more detail using a variety of molecular markers. In the first series of experiments, genes expressed in the axial and paraxial mesoderm were examined. The expression of the *goosecoid* gene, which marks the first involuting cells of the gastrula and the most dorsal-anterior mesoderm (Stachel et al., 1993; Schulte-Merker et al., 1994), appears normal at shield stage in class 3, 4 and 5 (*pgy, snh*, and *swr*) mutant embryos (Fig. 4J-M and data not shown). Thus the most anterior axial mesoderm appears normal.

The more posterior axial mesoderm of the notochord is expanded laterally; however, the primary cause of this expansion appears to be a reduced amount of dorsal convergence. In strong and intermediate phenotypes (classes 3, 4 and 5), the enlargement of the notochord, which is visible in live embryos, was confirmed by analyzing the expression pattern of Ntl (Schulte-Merker et al., 1992) in mutant embryos at the bud stage (Fig. 3A-D). By this stage in wild type, the notochord precursors have formed 2 layers of cells as a result of dorsal convergence. In class 5 mutant embryos (*swr*) at this stage, only a single layer of cells is observed for most of the notochord anlage and the anlage is shortened in its anterior-posterior length. Indeed counting the number of Ntl-positive nuclei in wild type and *swr* mutant embryos reveals that the majority of the broadened midline in *swr* is due to a reduced amount of dorsal convergence and extension and not to an increased number of notochord precursors.

In the mutant embryos, a mediolateral expansion of adaxial cells is revealed by *myoD* expression (Weinberg et al., 1996). In wild type at bud stage, *myoD* is expressed in 2 stripes of paraxial mesoderm (Fig. 3E′, Weinberg et al., 1996), which correspond to the adaxial cells (Felsenfeld et al., 1991; Thisse et al., 1993). The adaxial cells form 4 rows of cells, one on top of the other, which lie directly adjacent to the notochord (M. Westerfield and S. Devoto, personal communication). This 1-2 cell wide region in wild-type embryos (Weinberg et al., 1996; Fig. 3E′) is broadened to 4-5 cells in width in class 5 (*swr*), 3-4 cells in class 4 (*snh*), and 2-3 cells in class 3 (*pgy*) embryos (Fig. 3F′-H′). In addition, in mutant embryos *myoD* is strongly expressed posteriorly in an adjoining half-ring in the tailbud, which is not seen in the wild type (Fig 3E-H). The anterior-posterior length of the adaxial expression is shorter in class 3, 4 and 5 embryos than in wild-type embryos (Fig. 3E-H), in parallel to the shortened notochord region. The mediolateral expansion of *myoD* in the mutants may be due to a reduced amount of dorsal convergence, rather than an enlarged population of adaxial cells. In class 2 (*laf*) mutant embryos the adaxial *myoD* expression looks normal at the bud stage (data not shown).

At the 5-6 somite stage, *myoD* begins to be expressed more extensively in the somitic mesoderm (Weinberg et al., 1996) and is dramatically expanded in mutant embryos, consistent with the morphology seen in live embryos. In class 5 mutants (*swr* and *sbn*) all somites extend around the circumference of the embryo (Fig. 3M,N,P, data not shown). The first 2 somites in class 4 mutant embryos (*snh*) extend more laterally than in wild type, but do not reach the ventral side. However, somites posterior to somite 2, do extend around the circumference (Fig. 3Q,R). In class 3 embryos (*pgy*) the first 5 somites extend about twice the length laterally as the equivalent wild-type somites (Fig. 3S,T), while in the case of class 2 mutant embryos (*laf*), *myoD* expression is broadened only in the tail (Fig. 3I,J). Since the anterior somitic mesoderm is derived from laterally positioned cells in the blastoderm (Kimmel et al., 1990; Shih and Fraser, 1995), a reduced amount of dorsal convergence cannot be the cause of the ventrally located somites in class 5 and 4 (*swr*, *sbn* and *snh*) mutant embryos. The expanded somitic *myoD* expression in these mutants is likely due to an enlarged population of somitic mesodermal cells. For class 2 and 3 mutants (*laf* and *pgy*), determination of the number of somitic mesodermal cells is necessary to assess whether this population of cells is enlarged.

Reduced domains of ventrally expressed genes

We investigated whether the expansion of the dorsal-lateral mesoderm is accompanied by a reciprocal reduction of cell types normally derived from ventral regions. We examined the expression of the *gata1* gene (Detrich et al., 1995), normally expressed in the blood precursors, mesodermal cells known to arise from a ventral region in the zebrafish blastoderm fate map (Kimmel et al., 1990; Lee et al., 1994; Stainier et al., 1993). At the 8 somite stage, *gata1* is expressed in 2 lateral stripes that fuse in a ventral position, just posterior to the tailbud (Fig. 4A,B). In mutant embryos *gata1* expression is absent or reduced. In all class 5 (*swr*) and most class 4 (*sbn* and *snh*) mutant embryos examined, no *gata1* expressing cells were detectable (Fig 4C-F, data not shown). However, a small domain of expression is sometimes observed in class 4 mutant embryos (Fig 4G, data not shown). In class 3 (*pgy*) mutants, the *gata1* expression domain is shortened along its anterior-

posterior length (Fig. 4H), while the width of the expression domain is normal, indicating a reduced number of cells expressing *gata1* in class 3 embryos. The *gata1* expression results are consistent with the absence or reduction of blood found in these mutant embryos in a histological stain (data not shown). In class 2 (*laf*) mutant embryos, *gata1* expression looks normal at the 8 somite stage (Fig. 4I).

The expression of *eve1*, a marker of ventral and lateral regions at early gastrula stages (Joly et al., 1993), is reduced in class 5 and 4 mutant embryos (*swr* and *snh*). At shield stage *eve1* expression is strongly reduced in class 5 mutant embryos (Fig. 4J,K). In class 4 mutant embryos a moderate reduction in *eve1* is apparent at 70% epiboly (Fig. 4L,M). The extent of the expression domain appears normal in both class 4 and 5 embryos, but the amount of expression is decreased. It appears that the level expressed in dorsolateral regions is extended to the ventral midline. This is consistent with the expansion of anterior somites, which are derivatives of dorsolateral cells of the blastoderm, to ventral positions. A reduction in *eve1* expression is also seen in class 3 (*pgy*) and class 2 (*laf*) mutant embryos at the 5 somite stage (data not shown).

The neural plate extends circumferentially in *swr* and is expanded in *snh* mutant embryos

In *Xenopus*, signals involved in the dorsalization of the mesoderm also play a role in neural induction, while signals ventralizing the mesoderm repress neural induction processes (Hawley et al., 1995; Sasai et al., 1995; Wilson and Hemmati-Brivanlou, 1995). In order to investigate whether the expansion of dorsal fates in the mesoderm is linked to an enlargement of the presumptive neural region, we examined the expression of *fkd3* and *pax*2.

fkd3 is expressed dorsally in the presumptive neuroectoderm at early gastrulation stages (J.O., unpublished) (Fig. 4N). In class 5 (*swr*) mutant embryos *fkd3* expression is no longer limited to dorsal regions at 70% epiboly, but instead encircles the circumference of the embryo (Fig. 4O). In class 4 (*snh*) embryos the domain is expanded to ventrolateral regions (Fig. 4P). These results clearly show an expansion of neuroectoderm in class 4 and 5 mutant embryos.

In wild-type embryos at the 10 somite stage, *pax2* (formerly *paxb*) is expressed in a variety of cell types, which include the optic stalk, parts of the optic vesicle, the otic placode, the posterior part of the midbrain, isolated neuronal precursors of the hindbrain and spinal cord, and the ventrolateral mesodermal progenitors of the pronephros (Fig. 4Q; Krauss et al., 1991a). Strikingly, in 10 somite stage class 5 mutant embryos (*swr*) the midbrain expression domain of *pax2* extends around the entire circumference of the embryo (Fig. 4R). The optic vesicle expression is present in the middle of the ring of *pax2* staining; it does not lie superficially as in wild type, but deep in a mass of tissue. This is consistent with morphological observations at this stage where the optic placodes come to lie in a ball of tissue at the animal pole (data not shown). The otic vesicle, pronephric, and neuronal precursor expression are not visible in class 5 mutant embryos (Fig. 4R). However, small amounts of sporadic *pax2* expression are seen in posterior ventral and ventrolateral regions, which could correspond to any one of these cell types (data not shown).

In class 4 mutant embryos (*snh*) the optic vesicle expression of *pax2* appears normal, however, all the posterior expression domains are altered (Fig. 4S). The midbrain expression is broadened to about 3 times its width in wild type. The presumptive otic vesicle expression of *pax2* lying posterior to the midbrain is not visible. Patches of stained cells appear to be spread out laterally over the yolk consistent with the morphology in 2-day old embryos where the otic vesicles are found fragmented on the yolk (data not shown). The two stripes of neuronal staining in the spinal cord are present but lie in more lateral positions than in wild type, probably due to an enlarged neural plate. In addition, more neuronal precursor cells are observed. The pronephric expression of *pax2* is reduced to a small patch on the yolk lying just posterior to the twisted axis.

In class 3 (*pgy*) mutant embryos the anterior *pax2* expression domains of the optic vesicle, midbrain, otic placode and neuronal precursors appear normal (Fig. 4T). The pronephric expression domain, however, is altered in two ways. First it is shortened in its anterior-posterior length, but in addition the stripes are broadened mediolaterally in class 3 mutant embryos. It is difficult to interpret the meaning of this result. In class 2 (*laf*) mutant embryos, *pax2* expression appears normal (Fig. 4U).

Genetic features

Several of the genes produce both recessive and dominant phenotypes, as well as variability in the mutant phenotype.

swr^{ta72} shows a dominant zygotic phenotype

swr^{ta72} displays dominant class 1 and 2 zygotic phenotypes at varying frequencies (Table 2, Fig. 2J). It is likely that the penetrance of the dominant phenotype is dependent on the genetic background, as in our recent generation of fish that had undergone several outcrosses, almost no dominance is observed. In reciprocal crosses, a maternal influence on the frequency or strength of the dominant phenotype is not obvious. All embryos displaying a dominant phenotype that survived and were fertile, were heterozygous for the mutation (18/18 fish).

pgy shows a dominant zygotic-maternal phenotype

A dominant phenotype is also observed in *pgy*. In this case, the dominant embryonic phenotype is displayed only if both the maternal and zygotic genotypes are heterozygous for the mutation. About 50% of the embryos of crosses between heterozygous females with the strongest *pgy* allele, *pgy*^{dty40}, and wild-type males display class 1 and 2 phenotypes. No dominant phenotype is observed in the progeny of *pgy*^{dty40}/+ males crossed to wild-type females, while 50% of the embryos show the dominant phenotype in intercrosses between two heterozygous parents (Table 2). Many of the embryos with weak defects survive to adulthood and of the 36 adults tested, all were *pgy*^{dty40} heterozygotes. A similar genetic behavior of zygotic-maternal dependence is observed in the epiboly mutants described by Kane et al. (1996).

The dominant ventral tail fin phenotypes observed in *swr* and *pgy* mutant embryos are likely due to partial loss of function of these genes, as opposed to a gain-of-function defect. This is clearest with *pgy* for which 6 alleles were found, 3 of which are completely recessive and also show the weakest homozygous phenotypes resulting from the 6 alleles. As the strength of the recessive phenotype increases for the 3 strongest alleles, so does the strength and penetrance of the

Fig. 3. Ntl and *myoD* expression in *swr*, *snh*, *pgy* and *laf* mutant embryos. Animal pole or anterior is left or up, except where noted. A dorsal view of whole-mount anti-Ntl antibody stainings at the bud stage of wild type (A); *swr* (B) where the Ntl notochord domain is about twice as broad as in wild type; *snh* (C) where the Ntl domain is about 50% broader than in wild type; and *pgy* (D) where the Ntl domain is about 25% broader than in wild type. In E-H,S,T the yolk was removed and then the axis of the embryo flattened onto a slide in order to visualize the entire axis of the embryo (a 'spread'). Spreads of *myoD* in situ hybridizations of bud stage embryos in wild type (E,E′), *swr* (F,F′), *snh* (G,G′), and *pgy* (H,H′) mutant embryos. Higher magnifications of the posterior expression (E′–H′) show the mediolateral expansion of *myoD* expression. Lateral view of a whole-mount *myoD* staining at the 18-somite stage in wild-type (I) and *laf* mutant (J) embryos. An arrowhead indicates the enlarged somitic expression of *myoD* in *laf*. Dorsal (K,M,Q) and lateral (L,N,R) views of whole-mount *myoD* stainings of wild-type, *swr* and *snh* embryos at the 6-7 somite stage. From a dorsal view of *snh* (Q) 7 somites are visible. In a lateral view of the same *snh* embryo (R), it is apparent that only the 5 most posterior somites extend around the circumference of the embryo. Spreads of *myoD* staining at the 5-6 somite stage in wild type (S) and *pgy* (T). The wild-type embryo (K) is shown from the vegetal pole (O). In P a vegetal pole view of the *swr* embryo in M shows the first two somites extending around the circumference of the embryo. The more posterior somites also extend to the ventral side and fuse, but are not in the plane of focus.

dominant zygotic-maternal phenotype (Table 2), which appears identical to the recessive phenotypes produced by other *pgy* alleles. These data along with the gradation in homozygous phenotypes displayed by mutants with the 6 *pgy* alleles strongly suggest that the dominant phenotypes are a result of a partial loss of function of the *pgy* gene product. Thus proper development of the embryo is very sensitve to the dosage of the *pgy* gene product.

sbn exhibits a dominant maternal and zygotic phenotype

A mutation with unique properties, *sbn*, produces a completely penetrant dominant maternal-effect phenotype, where all progeny of heterozygous females crossed to wild-type males show a class 4 phenotype (Fig. 1I,J,K, Table 2). The progeny of a cross between a heterozygous male and wild-type female also display a weak dominant zygotic class 1 or 2 phenotype of varying penetrance (Table 2). Homozygous *sbn* embryos develop the strongest phenotype observed in our series (class 5).

Due to both the maternal and zygotic dominance of *sbn*, complementation tests have not been conclusive. Trans-heterozygous *swr/sbn* embryos show phenotypes stronger than the dominant zygotic, but weaker than the recessive phenotype of *swr* (Table 2). Interestingly, a cross between a pgy^{tc227a}/+ female and *sbn*/+ male shows a moderate class 3 phenotype, stronger than the recessive pgy^{tc227a} and dominant zygotic *sbn* phenotype (Table 2). *sbn* could be a very strong allele of *pgy* or an unusual allele of *swr*. Alternatively, *sbn* may be a gain- or loss-of-function mutation in an independent gene, which interacts with both *swr* and *pgy*. Due to the ambiguity in the complementation test results, we tentatively regard *sbn* as a distinct gene. Placing these mutations on the genetic map (Postlethwait et al., 1994) will clarify whether they are mutations in the same or different genes.

snh varies in its phenotypic strength

The only *snh* allele results in a strong recessive phenotype of little variance between embryos within the same egg lay. We observe, however, a variation in the phenotypic strength among

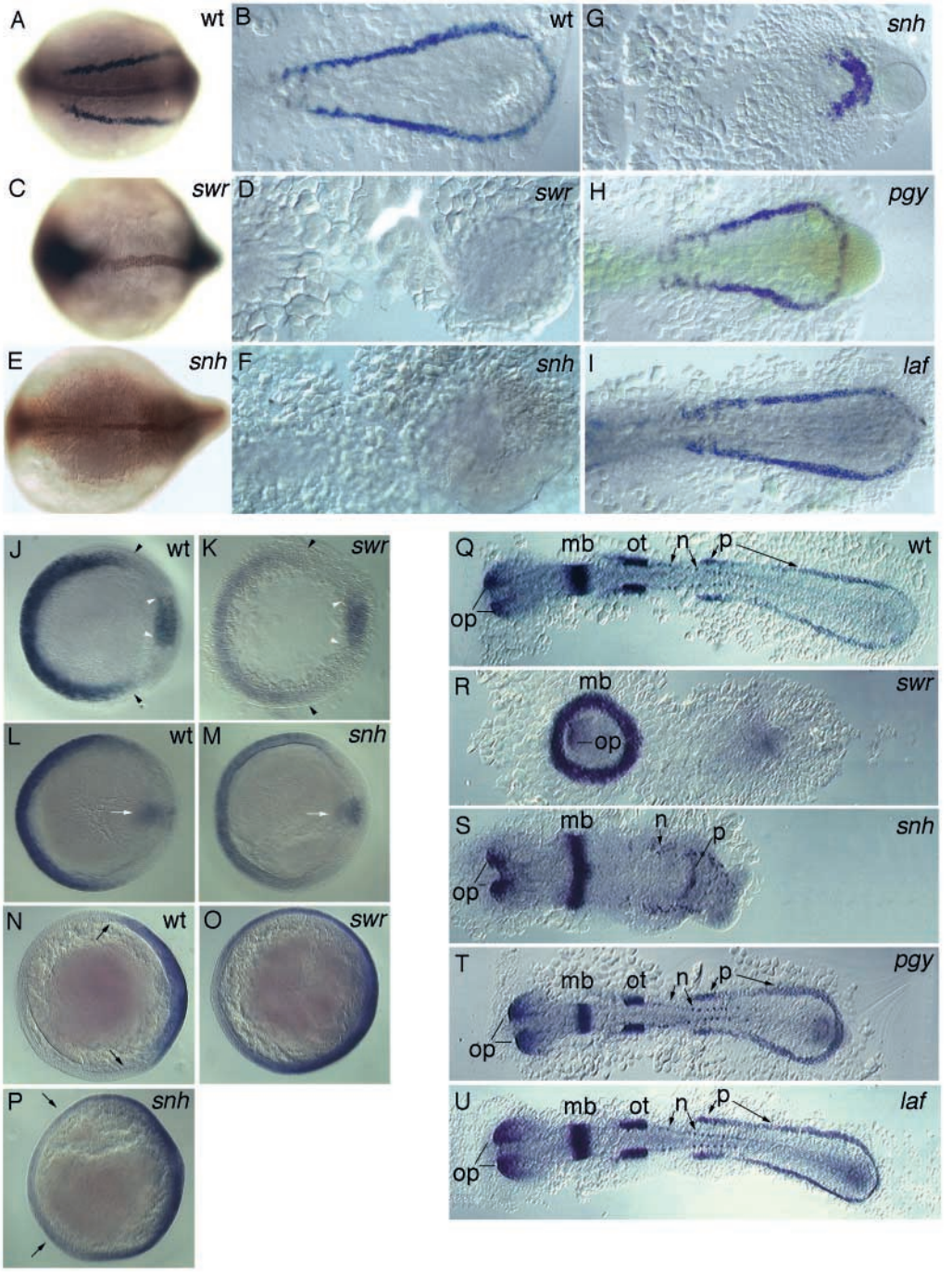

Fig. 4. Altered expression of *gata1*, *eve1*, *fkd3* and *pax2* in whole-mount in situ hybridizations of the dorsalized mutants. Expression of *gata1* in 8-somite stage wild-type embryos (A,B), *swr* (C,D), *snh* (E,F,G), *pgy* (H), and *laf* (I) mutant embryos. Double stainings with *gata1* and anti-Ntl antibody are shown as whole mounts in A,C,E. Spreads are shown in (B,D,F-I). *eve1*, *gsc* double staining at shield stage in wild-type (J) and *swr* mutant (K) embryos (white arrowheads delineate *gsc* expression). *eve1*, *gsc* double stainings at 70% epiboly in wild-type (L), and *snh* mutant (M) embryos (white arrow marks *gsc* expression). *fkd3* expression at 70% epiboly in wild-type (N), *swr* mutant (O), and *snh* mutant (P) embryos (black arrows indicate the lateral extent of staining). Spreads of *pax2*-stained 10-somite stage wild type (Q), *swr* (the most anterior position of the embryo lies in the middle of the ring; R), *snh* (S), *pgy* (T), and *laf* (U) mutant embryos. op, optic vesicle and stalk; mb, midbrain; ot, otic vesicle; n, neuronal and p, pronephric precursor expression domains.

individual fish (Table 2, note the class 3 phenotype in one *snailhouse* cross and class 4 phenotype in two crosses). This is probably due to differences in genetic background.

DISCUSSION

In our large-scale screen for visible embryonic mutants, we identified a total of 22 mutants displaying expansions of tissues normally derived from dorsolateral cells of the blastoderm at the expense of ventrally derived cell types. These mutants all have similar phenotypes, although the extent to which each particular mutant is affected differs. The phenotypic spectrum observed ranges from a very weak defect restricted to the posterior of the embryo to a dramatic expansion of dorsolaterally derived structures around the entire circumference of the embryo. The genetic parameters of these mutants indicate that both maternal and zygotic contributions are required for establishing proper dorsoventral pattern formation in the zebrafish embryo and that they are required in a dosage sensitive process.

The altered expression domains demonstrate a dorsalization of the embryo

A partial dorsalization of the embryo is reflected in the

reduction of expression of ventrally expressed genes accompanied by the ventrolateral expansion of normally dorsally restricted gene expression. In class 4 and 5 mutant embryos, *eve1* expression is decreased and the *pax2* pronephric and *gata1* blood precursor expression is absent or reduced, demonstrating a reduction of cell types derived from ventral regions of the blastoderm. The paraxial mesoderm is expanded, with the effect on the adaxial cells being less pronounced than on the somitic mesoderm, which extends to the ventral side. Only a slight enlargement of the posterior axial mesoderm is observed, while the region expressing *goosecoid*, the anterior axial mesoderm, does not appear enlarged. The dorsally derived neuroectoderm is expanded to ventrolateral regions. Although this has to be confirmed with more molecular markers, it appears that there is a progression in the strength of the defects from dorsal to ventral positions, with the most dorsal positions the least affected. The altered expression patterns at very early gastrulation stages indicate that the primary defect in these mutants is in pattern formation, as opposed to morphogenesis. The data together demonstrate a dorsalization phenotype in *swr, snh*, and *sbn* mutant embryos (classes 5 and 4) where pattern formation is affected along most of the dorsoventral axis. In *pgy, laf* and *mfn* mutant embryos (classes 3, 2 and 1) the dorsalization is less dramatic and restricted to more posterior regions. The phenotypic series of the dorsalized mutants suggests the involvement of a gradient determining position along the dorsoventral axis.

At least 5 genes are essential for the specification of ventral cell types in the zebrafish

We identified 5 clearly independent genes, *swr, snh, pgy, laf* and *mfn*, which are required for specification of ventral regions in the zebrafish embryo. Due to the dominance of *sbn* and its strong genetic interaction with both *pgy* and *swr*, it is difficult to assess its allelism and so we tentatively consider it a sixth gene. Multiple alleles were isolated for *swr, pgy*, and *mfn* genes, while only a single allele was found for *snh, sbn*, and *laf*. Complementation testing is incomplete for 3 mutations (Table 1). Homozygous mutant *swr* and *sbn* embryos show the strongest phenotype (class 5) followed by those of *snh* (class 4) and *pgy* (class 3). The weakest defects are seen in *laf* (class 2) and *mfn* (class 1) mutant embryos. For none of these genes do we know if a null mutation exists, although it appears that all of the mutations are loss-of-function alleles, with the possible exception of *sbn*. Three of the genes, *pgy, sbn* and *swr* show dominant zygotic phenotypes. These dominant defects, which consist of reductions in ventral tail tissues, are semi-lethal and consequently result in a selective disadvantage in the propagation of the mutation. Thus, null or strong loss-of-function mutations of *pgy, sbn* and *swr* may have been selected against in our inbreeding scheme (Mullins et al., 1994) and therefore may be underrepresented in our mutant collection.

A remarkable feature of *pgy*, and perhaps also *sbn*, is that it is required both maternally as well as zygotically for dorsoventral pattern formation. Due to the zygotic recessive lethality of the mutations, we were not able to raise homozygous mutant *pgy* females to look at the phenotype of the more complete loss-of-function of *pgy* (or *sbn*). Hence, the mutant phenotypes described are only partial loss-of-function phenotypes and the complete loss-of-function (which can be made by producing chimeric females containing homozygous mutant germline cells (Lin et al., 1992)) would show a more severe phenotype.

The dorsalized mutants resemble LiCl-treated dorsalized embryos

LiCl treatment of cleavage stage *Xenopus* or zebrafish embryos causes a dorsalization of the embryo. One class of LiCl-treated embryos in zebrafish, termed 'bustled' (Stachel et al., 1993), displays defects resembling the class 4 phenotype. Similar to these mutants the 'bustled' embryos have relatively normal dorsoanterior structures, an apparently enlarged notochord, and a twisted dorsoposterior axis lying above the yolk. During gastrulation some LiCl-treated embryos also resemble the dorsalized mutants in their ovoid shape at the bud stage, a posterior reduction in the circumference of the embryo in somite stages, and extension of the tailbud prematurely off the yolk. The defects are not identical, however, as the LiCl-treated embryos, for example, show an expanded domain of *goosecoid* expression.

The most dorsalized class of LiCl-treated zebrafish embryos, in which multiple dorsal axes are formed ('radialized' embryos), was not seen in our mutant collection. It is likely that this is in part due to the residual maternal (and possibly also zygotic) component of *pgy* or another maternally functioning gene(s) that contributes to dorsoventral patterning. Alternatively, LiCl may disrupt the function of multiple pathways involved in pattern formation of the early embryo, which could not be mimicked by the loss of a single gene product.

The genes described here are candidates for components of a ventralization pathway

The similar and overlapping phenotypes found for mutations in these 6 genes suggest that they function in the same pathway. *swr* and *sbn* function early in the embryo and phenotypic effects are visible as early as the shield stage. *snh* and *pgy* function by late gastrulation stages, while *laf* and *mfn* may be acting only late in the dorsoventral patterning of the tail, along with the other genes. All these genes are candidates for a ventralizing molecule that opposes the dorsalizing signal emanating from the Spemann organizer. The phenotypes of these mutants are those expected from a mutation in a component of a ventralization pathway. In the dorsalized mutant embryos, the activity of the dorsal signal would extend to more ventral regions due to a loss of its repression by a ventralizing factor. Possibly, a graded activity emanating from the Spemann organizer could be repressed by a nongraded or graded ventralizing molecule. The products of the 6 genes identified here could be the ventralization factor itself or could be involved in generating or executing its function.

A reduction in a single factor in *swr* and *snh* could account for both the expansion of dorsal mesoderm and neuroectoderm observed in these mutant embryos. In *Xenopus*, the ectopic expression of *BMP-4* leads to the ventralization of dorsal mesoderm and to the repression of neural differentiation and the induction of epidermal cell fates (Dale et al., 1992; Jones et al., 1992; Schmidt et al., 1995a; Sasai et al., 1995; Wilson and Hemmati-Brivanlou, 1995), while a dominant negative form of *BMP-4* has the opposite effect (Hawley et al., 1995). In *swr* mutant embyros the neural plate extends around the circumference of the embryo and in *snh* it is expanded laterally. The

inductive and repressive properties of *BMP-4* in *Xenopus* would predict that the expansion in neuroectoderm in *swr* and *snh* occurs at the expense of epidermis. This has not yet been tested.

Several cloned genes are candidates for the genes described here. *wnt8*, which has ventralizing effects in *Xenopus* embryos when expressed after the midblastula stage (Christian and Moon, 1993), and *eve1*, are expressed zygotically in ventral and lateral regions (Christian and Moon, 1993; Joly et al., 1993) and are candidates for *swr*, *snh*, *laf*, and *mfn*. In *Xenopus*, *BMP-4*, the BMP receptor (Graff et al., 1994), and *gsk-3* (He et al., 1995; Pierce and Kimelman, 1995) and *wnt8* in zebrafish (Kelly et al., 1995) are expressed maternally and zygotically making them candidates for *sbn* and *pgy* and possibly also *swr*, *snh*, *laf*, and *mfn*. The maternal components of *pgy* and *sbn* make them candidates for the blastula stage vegetal signal that induces ventral mesoderm (the ventral counterpart of the Nieuwkoop center). *BMP-4* and *gsk-3* have ventral mesoderm-inducing abilities (He et al., 1995; Pierce and Kimelman, 1995) and thus are candidates for this signal and for *pgy* and *sbn*. Isolation of the zebrafish homologues of these genes, followed by a linkage analysis between the genes and the mutations will identify if any of these cloned genes correspond to the genes described here. This work is currently in progress.

The dorsalized mutant phenotypes are complementary to the ventralized defects of *dino* and *mercedes*

Two genes we identified in our large-scale screen, *dino* and *mercedes*, result in ventralized phenotypes reciprocal to those found in dorsalized mutant embryos (Hammerschmidt et al., 1996). *dino* mutant embryos have a reduced head and trunk, an increased number of blood cells, an enlarged tail, and multiple ventral tail fins. These defects are in striking contrast to the dorsalized phenotypes described here, suggesting that the 2 groups of genes function antagonistically. Double mutant combinations between the ventralized and dorsalized mutants will reveal the relationships between these 2 groups of genes in dorsoventral pattern formation.

Dorsoventral patterning in vertebrates and invertebrates

In *Drosophila* at least 7 genes function zygotically in setting up the dorsoventral axis. Two of these genes, *short gastrulation* (*sog*) and *decapentaplegic* (*dpp*), function antagonistically to each other in establishing pattern in the dorsal region of the *Drosophila* embryo (Ferguson and Anderson, 1992; Wharton et al., 1993; François et al., 1994). Related genes to *sog* (François et al., 1994) and *dpp* (Padgett et al., 1987) in *Xenopus*, *chordin* (Sasai et al., 1994; François and Bier, 1995) and *BMP-4*, respectively, function in an opposite manner to their *Drosophila* counterparts: *chordin* is a dorsalizing factor (Sasai et al., 1994), while *BMP-4* is ventralizing. *dpp* has been shown to function in a similar manner to *BMP-4* in promoting ventral cell fates in ectopic expression experiments in *Xenopus* (Holley et al., 1995). Likewise, human *BMP-4* can substitute for *dpp* in *Drosophila* (Padgett et al., 1993). These and other studies have provided molecular evidence for an old hypothesis that the dorsoventral axis is inverted between vertebrates and arthropods (Nübler-Jung and Arendt, 1994; Holley et al., 1995; Schmidt et al., 1995b; Hogan, 1995; De Robertis and Sasai, 1996).

In *Drosophila dpp* acts as a morphogen in establishing the positional information in the dorsal half of the embryo. Highest activities determine the most dorsal cell fates, intermediate levels dorsolateral cell types, and the lowest activities are necessary for lateral cell fate specification (Ferguson and Anderson, 1992; Wharton et al., 1993). *dpp* function is very sensitive to its gene dosage. Null alleles of *dpp* show dominant zygotic lethality, producing embryos with a weakly ventralized phenotype (Irish and Gelbart, 1987). The parallels between the loss-of-function defects of *dpp* in *Drosophila* and those of the dorsalized mutants in zebrafish are worth noting. Both display a phenotypic series, show dominant defects and are extremely sensitive to gene dosage. It is tempting to speculate that *BMP-4* functions in a similar manner in vertebrates to *dpp* in *Drosophila* and that the genes we identified here are functional components of a pathway where *BMP-4* acts as a morphogen to establish ventral positional information in the zebrafish embryo.

We would like to thank: Eric Weinberg, and David Ransom and Leonard Zon for providing the *myoD* and *gata1* cDNA clone, respectively, prior to publication; David Ransom for pointing out the histological blood staining method; J. S. Joly for the *eve1* cDNA clone; Mary Ellen Lane, Siegfried Roth, Stefan Schulte-Merker, Herbert Steinbeiser for helpful comments on the manuscript; and very special thanks to Karin Finger-Miller for technical support, as well as to Hans-Martin Maischein, Amanda Wilson, Jörg Zeller, and Cosima Fabian. This work was supported by an NIH postdoctoral fellowship to M. C. M.

REFERENCES

Ang, S. L. and Rossant, J. (1994). HNF-3 beta is essential for node and notochord formation in mouse development. *Cell* **78,** 561-574.

Beddington, R. S., Rashbass, P. and Wilson, V. (1992). Brachyury – a gene affecting mouse gastrulation and early organogenesis. *Development* **Supplement** 157-165.

Christian, J. L. and Moon, R. T. (1993). Interactions between Xwnt-8 and Spemann organizer signaling pathways generate dorsoventral pattern in the embryonic mesoderm of *Xenopus*. *Genes Dev.* **7,** 13-28.

Conlon, F. L., Lyons, K. M., Takaesu, N., Barth, K. S., Kispert, A., Hermann, B. and Robertson, E. J. (1994). A primary requirement for *nodal* in the formation and maintenance of the primitive streak in the mouse. *Development* **120,** 1919-1938.

Cui, Y., Brown, J. D., Moon, R. T. and Christian, J. L. (1995). *Xwnt-8b*: a maternally expressed *Xenopus Wnt* gene with a potential role in establishing the dorsoventral axis. *Development* **121,** 2177-2186.

Dale, L., Howes, G., Price, B. M. J. and Smith, J. C. (1992). Bone morphogenetic protein 4: a ventralising factor in *Xenopus* development. *Development* **115,** 573-585.

Dale, L. and Slack, J. M. W. (1987). Fate map for the 32-cell stage of *Xenopus laevis*. *Development* **99,** 527-551.

Deng, C. X., Wynshaw-Boris, A., Shen, M. M., Daugherty, C., Ornitz, D. M. and Leder, P. (1994). Murine FGFR-1 is required for early postimplantation growth and axial organization. *Genes Dev.* **8,** 3045-57.

De Robertis, E. M. and Sasai, Y. (1996). A common plan for dorsoventral patterning in Bilateria. *Nature* **380**, 37-40.

Detrich, H. W., Kieran, M. W., Chan, F. Y., Barone, L. M., Yee, K., Rundstadler, J. A., Pratt, S., Ransom, D. and Zon, L. I. (1995). Intraembryonic hematopoietic cell migration during vertebrate development. *Proc. Nat. Acad. Sci. USA* **92**, 10713-10717.

Devillers, C. (1952). Coordination des forces épiboliques dans la gastrulation de *Salmo*. *Bull. Soc. Zool. Fr.* **77,** 304-309.

Fainsod, A., Steinbeisser, H. and De Robertis, E. M. (1994). On the function of *BMP-4* in patterning the marginal zone of the *Xenopus* embryo. *EMBO J.* **13,** 5015-5025.

Felsenfeld, A. L., Curry, M. and Kimmel, C. B. (1991). The fub-1 Mutation

Blocks Initial Myofibril Formation in Zebrafish Muscle Pioneer Cells. *Dev. Biol.* **148,** 23-30.

Ferguson, E. and Anderson, K. (1992). *Decapentaplegic* acts as a morphogen to organize dorsal-ventral pattern in the *Drosophila* embryo. *Cell* **71,** 451-461.

François, V. and Bier, E. (1995). Xenopus *chordin* and Drosophila *short gastulation* genes encode homologous proteins functioning in dorsal-ventral axis formation. *Cell* **80**, 19-20.

François, V., Solloway, M., O'Neill, J. W., Emery, J. and Bier, E. (1994). Dorsal-ventral pattening of the *Drosophila* embryo depends on a putative negative growth factor encoded by the *short gastrulation* gene. *Genes Dev.* **8**, 2602-2616.

Graff, J., Thies, R., Song, J., Celeste, A. and Melton, D. (1994). Studies with a *Xenopus* BMP receptor suggest that ventral mesoderm-inducing signals override dorsal signals in vivo. *Cell* **79,** 169-179.

Haffter, P., Granato, M., Brand, M., Mullins, M. C., Hammerschmidt, M., Kane, D. A., Odenthal, J., van Eeden, F. J. M., Jiang, Y.-J., Heisenberg, C.-P., Kelsh, R. N., Furutani-Seiki, M., Vogelsang, E., Beuchle, D., Schach, U., Fabian, C. and Nüsslein-Volhard, C. (1996). The identification of genes with unique and essential functions in the development of the zebrafish, *Danio rerio*. *Development* **123**, 1-36.

Hammerschmidt, M., Pelegri, F., Mullins, M. C., Kane, D. A., van Eeden, F. J. M., Granato, M., Brand, M., Furutani-Seiki, M., Haffter, P., Heisenberg, C.-P., Jiang, Y.-J., Kelsh, R. N., Odenthal, J., Warga, R. M. and Nüsslein-Volhard, C. (1996). *dino* and *mercedes*, two genes regulating dorsal development in the zebrafish embryo. *Development* **123**, 95-102.

Harland, R. M. (1994). The transforming growth factor beta family and induction of the vertebrate mesoderm: Bone morphogenetic proteins are ventral inducers. *Proc. Natl. Acad. Sci. USA* **91,** 10243-10246.

Hawley, S. H. B., Wünnenberg-Stapleton, K., Hashimoto, C., Laurent, M. N., Watabe, T., Blumberg, B. W. and Cho, K. W. Y. (1995). Disruption of BMP signals in embryonic *Xenopus* ectoderm leads to direct neural induction. *Genes Dev* **9,** 2923-2935.

He, X., Saint-Jeannet, J.-P., Woodgett, J., Varmus, H. and Dawid, I. (1995). Glycogen synthase kinase-3 and dorsoventral patterning in *Xenopus* embryos. *Nature* **374,** 617-622.

Hemmati-Brivanlou, A., Kelly, O. G. and Melton, D. A. (1994). Follistatin, an antagonist of activin, is expressed in the Spemann organizer and displays direct neuralizing activity. *Cell* **77,** 283-295.

Hemmati-Brivanlou, A. and Thomsen, G. H., (1995). Ventral mesodermal patterning in *Xenopus* embryos: Expression Patterns and activities of BMP-2 and BMP-4. *Dev. Genet.* **17**, 78-89.

Herrmann, B. G. and Kispert, A. (1994). The T genes in embryogenesis. *Trends Genet.* **10**, 280-286.

Ho, R. (1992). Axis formation in the embryo of the zebrafish, *Brachydanio rerio*. *Semin. Dev. Biol.* **3,** 53-64.

Hogan, B. L. M., Blessing, M., Winnier, G. E., Suzuki, N. and Jones, C. M. (1994). Growth factos in development: the role of TGF-ß related polypeptide signalling molecules in embryogenesis. *Development* **Supplement,** 53-60.

Hogan, B. L. M. (1995). Upside-down ideas vindicated. *Nature* **376**, 210-211.

Holley, S., Jackson, P., Sasai, Y., Lu, B., De Robertis, E., Hoffmann, F. and Ferguson, E. (1995). A conserved system for dorsal-ventral patterning in insects and vertebrates involving *sog* and *chordin*. *Nature* **376,** 249-253.

Irish, V. and Gelbart, W. (1987). The decapentaplegic gene is required for dorsal-ventral patterning of the *Drosophila* embryo. *Genes Dev.* **1,** 868-879.

Iuchi, I. and Yamamoto, M. (1993). Erythropoiesis in the developing rainbow trout, *salmo gairdneri deus*: histochemical and immunological detection of erythropoietic organs. *J. Exp. Zool.* **226,** 409-417.

Joly, J. S., Joly, C., Schulte-Merker, S., Boulekbache, H. and Condamine, H. (1993). The ventral and posterior expression of the zebrafish homeobox gene *eve1* is perturbed in dorsalized and mutant embryos. *Development* **119,** 1261-1275.

Jones, C. M., Lyons, K. M., Lapan, P. M., Wright, C. V. E. and Hogan, B. L. M. (1992). DVR-4 (Bone morphogenetic protein-4) as a posterior-ventralizing factor in *Xenopus* mesoderm induction. *Development* **115,** 639-647.

Kane, D. A., Hammerschmidt, M., Mullins, M. C., Maischein, H.-M., Brand, M., van Eeden, F. J. M., Furutani-Seiki, M., Granato, M., Haffter, P., Heisenberg, C.-P., Jiang, Y.-J., Kelsh, R. N., Odenthal, J., Warga, R. M. and Nüsslein-Volhard, C. (1996). The zebrafish epiboly mutants. *Development* **123**, 47-55.

Kelly, G. M., Greenstein, P., Erezyilmaz, D. F. and Moon, R. T. (1995). Zebrafish *wnt8* and *wnt8b* share a common activity but are involved in distinct developmental pathways. *Development* **121**, 1787-1799.

Kessler, D. and Melton, D. (1995). Induction of dorsal mesoderm by soluble, mature VG1 protein. *Development* **121,** 2155-2164.

Kessler, D. S. and Melton, D. A. (1994). Vertebrate embryonic induction: mesodermal and neural patterning. *Science* **266,** 596-604.

Kimmel, C. B., Ballard, W. W., Kimmel, S. R., Ullmann, B. and Schilling, T. (1995). Stages of embryonic development of the zebrafish. *Dev. Dyn.* **203,** 253-310.

Kimmel, C. B., Warga, R. M. and Schilling, T. F. (1990). Origin and organization of the zebrafish fate map. *Development* **108,** 581-94.

Kimelman, D., Christian, J. L. and Moon, R. T. (1992). Synergistic principles of development: overlapping patterning systems in *Xenopus* mesoderm induction. *Development* **116**, 1-9.

Köster, M., Plessow, S., Clement, J. H., Lorenz, A., Tiedemann, H. and Knochel, W. (1991). Bone morphogenetic protein 4 (*BMP-4*), a member of the TGF-beta family, in early embryos of *Xenopus laevis*: analysis of mesoderm inducing activity. *Mech. Dev.* **33,** 191-9.

Kostomarova, A. A. (1969). The differentiation capactiy of isolated loach (*Misgurnis fossilis* L.) blastoderm. *J. Embryol. Exp. Morphol.* **22,** 407-430.

Krauss, S., Johansen, T., Korzh, V. and Fjose, A. (1991a). Expression of the zebrafish paired box gene pax(zf-b) during early neurogenesis. *Development* **113,** 1193.

Krauss, S., Johansen, T., Korzh, V. and Fjose, A. (1991b). Expression pattern of zebrafish pax genes suggests a role in early brain regionalization. *Nature* **353,** 267-270.

Ku, M. and Melton, D. (1993). *Xwnt-11*: a maternally expressed *Xenopus wnt* gene. *Development* **119,** 1161-1173.

Lamb, T. M., Knecht, A. K., Smith, W. C., Stachel, S. E., Economides, A. N., Stahl, N., Yancopolous, G. D. and Harland, R. M. (1993). Neural induction by the secreted polypeptide noggin. *Science* **262,** 713-8.

Lee, R., Stainier, D., Weinstein, B. and Fishman, M. (1994). Cardiovascular development in the zebrafish. II. Endocardial progenitors are sequestered within the heart field. *Development* **120,** 3361-3366.

Lin, S., Long, W., Chen, J. and Hopkins, N. (1992). Production of germ-line chimeras in zebrafish by cell transplants from genetically pigmented to *albino* embryos. *Proc. Natl. Acad. Sci. USA* **89,** 4519-4523.

Maeno, M., Ong, R. C., Suzuki, A., Ueno, N. and Kung, H. (1994). A truncated bone morphogenetic protein receptor alters the fate of ventral mesoderm to dorsal mesoderm: roles of animal pole tissue in the development of the ventral mesoderm. *Proc. Natl. Acad. Sci. USA* **91**, 10260-10264.

Mishina, Y., Suzuki, A., Ueno, N. and Behringer, R. R. (1995). Bmpr encodes a type I bone morphogenetic protein receptor that is essential for gastrulation during mouse embryogenesis. *Genes Dev.* **9,** 3027-3037.

Mullins, M. C., Hammerschmidt, M., Haffter, P. and Nüsslein-Volhard, C. (1994). Large-scale mutagenesis in the zebrafish: in search of genes controlling development in a vertebrate. *Curr. Biol.* **4,** 189-202.

Nübler-Jung, K. and Arendt, D. (1994). Is ventral in insects dorsal in vertebrates?. *Roux Arch. Dev. Biol.* **203,** 357-366.

Oppenheimer, J. M. (1936). Structures developed in amphibians by implantation of living fish organizer. *Proc. Soc. Exp. Biol. Med.* **34,** 461-463.

Padgett, R. W., St. Johnston, R. D. and Gelbart, W. M. (1987). A transcript from a *Drosophila* pattern gene predicts a protein homologous to the transforming growth factor-β family. *Nature* **325**, 81-84.

Padgett, R. W., Wozney, J. M. and Gelbart, W. M. (1993). Human BMP sequences can confer normal dorsal-ventral patterning in the *Drosophila* embryo. *Proc. Natl. Acad. Sci. USA* **90**, 2905-2909.

Pierce, S. and Kimelman, D. (1995). Regulation of Spemann organizer formation by the intracellular kinase Xgsk-3. *Development* **121,** 755-765.

Postlethwait, J. H., Johnson, S. L., Midson, C. N., Talbot, W. S., Gates, M., Ballinger, E. W., Africa, D. andrews, R., Carl, T., Eisen, J. S., Horne, S., Kimmel, C. B., Hutchinson, M., Johnson, M. and Rodriguez, A. (1994). A genetic linkage map for the zebrafish. *Science* **264,** 699-703.

Sasai, Y., Lu, B., Steinbeisser, H. and De Robertis, E. (1995). Regulation of neural induction by the *Chd* and *BMP-4* antagonistic patterning signals in *Xenopus*. *Nature* **376,** 333-336.

Sasai, Y., Lu, B., Steinbeisser, H., Geissert, D., Gont, L. K. and De Robertis, E. M. (1994). *Xenopus chordin*: a novel dorsalizing factor activated by organizer-specific homeobox genes. *Cell* **79,** 779-90.

Schmidt, J. E., Suzuki, A., Ueno, N. and Kimelman, D. (1995a). Localized *BMP-4* mediates dorsal/ventral patterning in the early *Xenopus* embryo. *Dev. Biol.* **169**, 37-50.

Schmidt, J. E., François, V., Bier, E. and Kimelman, D. (1995b). *Drosophila short gastrualation* induces an ectopic axis in *Xenopus*: evidence for

conserved mechanisms of dorsal-ventral patterning. *Development* **121**, 4319-4328.

Schmitz, B. and Campos-Ortega, J. A. (1994). Dorso-ventral polarity of the zebrafish embryo is distinguishable prior to the onset of gastrulation. *Roux Arch. Dev. Biol.* **203,** 374-380.

Schulte-Merker, S., Hammerschmidt, M., Beuchle, D., Cho, K. W. and Robertis, E. M. D. (1994). Expression of zebrafish *goosecoid* and *no tail* products in wild type and mutant *no tail* embryos. *Development* **120,** 843-852.

Schulte-Merker, S., Ho, R. K., Herrmann, B. G. and Nüsslein-Volhard, C. (1992). The protein product of the zebrafish homologue of the mouse *T*-gene is expressed in nuclei of the germ ring and the notochord of the early embryo. *Development* **116,** 1021.

Shawlot, W. and Behringer, R. R. (1995). Requirement for Lim1 in head-organizer function. *Nature* **374,** 425-30.

Shih, J. and Fraser, S. E. (1995). Distribution of tissue progenitors within the shield region of the zebrafish gastrula. *Development* **121**, 2755-2765.

Sive, H. (1993). The frog prince-ss: A molecular formula for dorsoventral patterning in *Xenopus. Genes Dev.* **7,** 1-12.

Slack, J. M. W. (1994). Inducing factors in *Xenopus* early embryos. *Curr. Biol.* **4,** 116-126.

Smith, W. C. and Harland, R. M. (1991). Injected *Xwnt-8* RNA acts early in *Xenopus* embryos to promote formation of a vegetal dorsalizing center. *Cell* **67,** 753-65.

Smith, W. C., Knecht, A. K., Wu, M. and Harland, R. M. (1993). Secreted noggin protein mimics the Spemann organizer in dorsalizing *Xenopus* mesoderm. *Nature* **361,** 547-9.

Stachel, S. E., Grunwald, D. J. and Myers, P. Z. (1993). Lithium perturbation and goosecoid expression identify a dorsal specification pathway in the pregastrula zebrafish. *Development* **117,** 1261-1274.

Stainier, D. Y. R., Lee, R. K. and Fishman, M. C. (1993). Cardiovascular development in the zebrafish. 1. Myocardial fate map and heart tube formation. *Development* **119,** 31-40.

Steinbeisser, H., Fainsod, A., Niehrs, C., Sasai, Y. and De Robertis, E. M. (1995). The role of *gsc* and *BMP-4* in dorsal-ventral patterning of the marginal zone in *Xenopus*: a loss-of-function study using antisense RNA. *EMBO J.* **14**, 5230-5243.

Suzuki, A., Thies, R. S., Yamaji, N., Song, J. J., Wozney, J. M., Murakami, K. and Ueno, N. (1994). A truncated bone morphogenetic protein receptor affects dorsal-ventral patterning in the early *Xenopus* embryo. *Proc. Natl. Acad. Sci. USA* **91,** 10255-10259.

Thisse, C., Thisse, B., Schilling, T. F. and Postlethwait, J. H. (1993). Structure of the Zebrafish s*nail1* gene and its expression in wild-type, *spadetail* and *no-tail* mutant embryos. *Development* **119,** 1203-1215.

Warga, R. M. and Kimmel, C. B. (1990). Cell movements during epiboly and gastrulation in zebrafish. *Development* **108,** 569-80.

Weinberg, E. S., Allende, M. L., Kelly, C. L., Abdelhamid, A., Murakami, T. andermann, P., Doerre, G., Grunwald, D. J. and Riggleman, B. (1996). Developmental regulation of zebrafish *MyoD* in wild-type, *no tail* and *spadetail* embryos. *Development* **122,** 271-280.

Weinstein, D. C., Ruiz i Altaba, A., Chen, W. S., Hoodless, P., Prezioso, V. R., Jessell, T. M. and Darnell, J., Jr. (1994). The winged-helix transcription factor HNF-3 beta is required for notochord development in the mouse embryo. *Cell* **78,** 575-88.

Wharton, K. A., Ray, R. P. and Gelbart, W. M. (1993). An activity gradient of *decapentaplegic* is necessary for the specification of dorsal pattern elements in the *Drosophila* embryo. *Development* **117**, 807-822.

Wilson, P. and Hemmati-Brivanlou, A. (1995). Induction of epidermis and inhibition of neural fate by *BMP-4*. *Nature* **376,** 331-333.

Winnier, G., Blessing, M., Labosky, P. A. and Hogan, B. L. M. (1995). Bone morphogenetic protein-4 is required for mesoderm formation and patterning in the mouse. *Genes Dev.* **9,** 2105-2116.

Yamaguchi, T. P., Harpal, K., Henkemeyer, M. and Rossant, J. (1994). fgfr-1 is required for embryonic growth and mesodermal patterning during mouse gastrulation. *Genes Dev.* **8,** 3032-44.

(Accepted 25 May 1996)